



Aalborg Universitet

AALBORG UNIVERSITY
DENMARK

Hydraulic Characteristics of Seawave Slot-cone Generator Pilot Plant at Kvitsøy (Norway)

Margheritini, Lucia; Vicinanza, Diego; Kofoed, Jens Peter

Published in:
Proceedings of the 7th European Wave and Tidal Energy Conference

Publication date:
2007

Document Version
Publisher's PDF, also known as Version of record

[Link to publication from Aalborg University](#)

Citation for published version (APA):
Margheritini, L., Vicinanza, D., & Kofoed, J. P. (2007). Hydraulic Characteristics of Seawave Slot-cone Generator Pilot Plant at Kvitsøy (Norway). In *Proceedings of the 7th European Wave and Tidal Energy Conference: EWTEC 2007* European Ocean Energy Association.

General rights

Copyright and moral rights for the publications made accessible in the public portal are retained by the authors and/or other copyright owners and it is a condition of accessing publications that users recognise and abide by the legal requirements associated with these rights.

- Users may download and print one copy of any publication from the public portal for the purpose of private study or research.
- You may not further distribute the material or use it for any profit-making activity or commercial gain
- You may freely distribute the URL identifying the publication in the public portal -

Take down policy

If you believe that this document breaches copyright please contact us at vbn@aub.aau.dk providing details, and we will remove access to the work immediately and investigate your claim.

Hydraulic characteristics of seawave slot-cone generator pilot plant at Kvitsøy (Norway)

L. Margheritini¹, D. Vicinanza², J. P. Kofoed¹.

¹ Department of Civil Engineering, Aalborg University
Søhngårdsholmsvej 57, 9000 Aalborg, Denmark
E-mail: lm@civil.aau.dk

² Dipartimento di Ingegneria Civile, Seconda Università degli studi di Napoli
Via Roma 29, 81031 Aversa (CE), Italy
E-mail: diego.vicinanza@unina2.it

Abstract

This paper presents results on wave overtopping and loading on an innovative caisson breakwater for electricity production. The work reported here contributes to the European Union FP6 priority 6.1 (Sustainable Energy System). The design of the structure consists of three reservoirs one on the top of each other to optimize the storage of potential energy in the overtopping water. The wave loadings on the main structure can be estimated using experiences from breakwater design, but the differences between the structures is so large that more reliable knowledge is needed. Model tests were carried out to measure wave loadings and overtopping rates using realistic random 2D and 3D wave conditions; the model scale used was 1:60 of the SSG pilot at the selected location in the island of Kvitsøy, Norway. Pressure transducers were placed in order to achieve information on impact/pulsating loadings while in a second phase the model has been adapted and equipped with pumps to measure the overtopping flow rates in the single reservoirs. The results of the tests highlight differences between 2D and 3D conditions in terms of pressures and hydraulic efficiency.

Keywords: breakwaters, loadings, overtopping, SSG, 3D model tests.

and three reservoirs one on the top of each others (Figure 1) to optimize the storage of power in the overtopping waves (Kofoed, 2006; Vicinanza et al., 2006). The works for the construction of the structure will start in summer 2007 at the selected location in the island of Kvitsøy, Norway. The objective of the pilot project is to demonstrate at full-scale, the operation of one module of the SSG wave energy converter in a 19 kW/m wave climate, including turbine, generator and control system, and to connect the system to the public grid for electricity production. At this stage of development the wave energy sector needs reliable devices with a proved technology at a low cost. The SSG device will be built as a robust concrete structure and one of its future applications will be on breakwaters enabling sharing of costs. The purpose of the work described in this paper is to derive information on wave pressures/forces acting on sloping and vertical walls as well as on overtopping flow rates in 3D conditions. The overtopping results are used for geometrical optimization while the ones on loadings have been used for structural design as well as stability evaluation and have been presented at international level and for the certification of the pilot plant under construction.

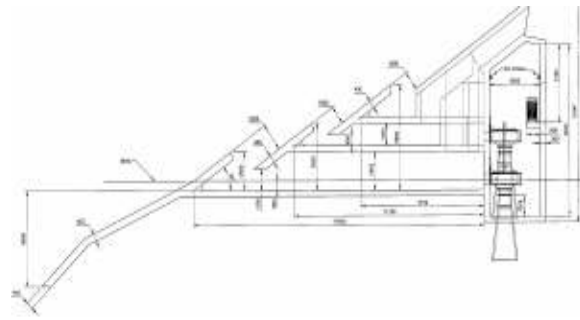


Figure 1: Section of the SSG pilot; on the rear part there is a dry room that will contain the turbines and generators; on the front, the apron and the 3 slopes designed to optimize the storage of the overtopping water to the three reservoirs. Reservoirs number: one the lower, two the middle and three the higher.

© Proceedings of the 7th European Wave and Tidal Energy Conference, Porto, Portugal, 2007

Introduction

The Sea Slot-cone Generator (SSG) is a wave energy converter (WEC) of the overtopping kind; it has a number of reservoirs one on the top of each others to optimize the capture on the potential energy in the overtopping water. It is a patented and certificated device developed by WAVEnergy, Stavanger, Norway. In 2008 the SSG pilot will be the first full scale wave energy converter producing electricity for the 520 inhabitants of Kvitsøy; the project regards a 150 kW onshore installation with approximately dimensions of 17 m (length) x 10 m (width) x 6 m (height)

1 Tests set up

Model tests have been performed in a wave tank at Aalborg University, in 1:60 length scale compared to the prototype. This wave basin is a steel bar reinforced concrete tank with the dimensions 15.7 x 8.5 x 1.5 m. The paddle system is a snake-front piston type with a total of ten actuators, enabling generation of short-crested waves. The waves are absorbed by a rubble beach slope in the back of the basin to minimize reflection.

The wave generation software used for controlling the wave paddles is AWASY5, developed by the laboratory research staff. The bathymetry in the immediate proximity of the pilot plant has been surveyed and the results have been used as the basis for the laboratory model. The SSG caisson model was built in plexiglas with dimension of 0.471 x 0.179 m (Figure 2).



Figure 2: SSG caisson model.



Figure 3: Plexiglas model on the reproduction of the cliff at Kvitsøy; in front the seven resistive probes.

The three front plates were positioned with a slope of $\alpha = 35^\circ$. The model was fixed rigidly on a 3D concrete model of the cliff located in the middle of the basin at 5 m

from the paddles. Seven resistive wave probes were located on a pentangle array placed on the plateau (Figure 3). Fourteen Kulite Semiconductor pressure cells were used to measure the pressure in a total of 25 positions on the structure plates. Two different transducer configurations were needed because of the very limited space inside the model combined with the physical dimensions of the pressure transducers (Fig. 4).

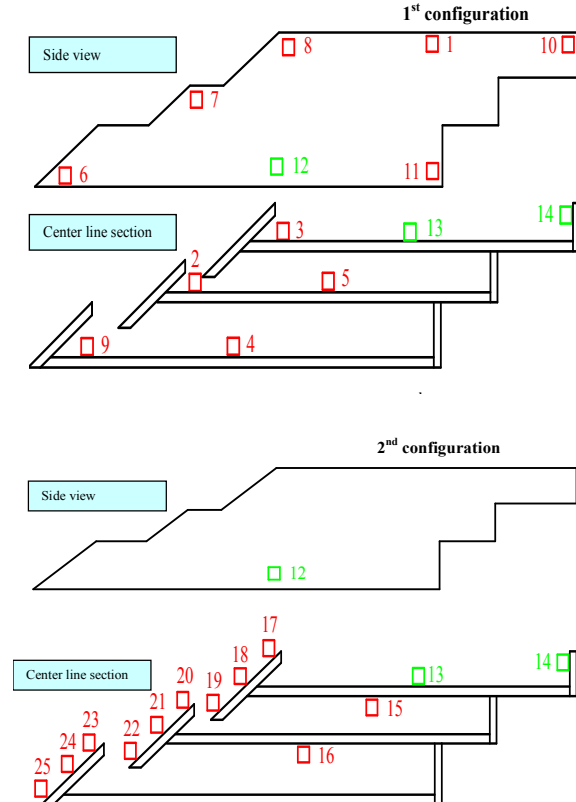


Figure 4: Test configuration and pressure cells locations (green identify transducers locations used in both configurations).

Table 1 shows the JONSWAP sea states selected for the tests. Each test comprised approximately 1000 waves. Tests were carried out with frontal and oblique waves (45° , denoted “Side”), with various levels of directional spreading (n).

The experimental procedure has been designed to ensure that data are available to allow a good estimation of the surface loads corresponding to the design 100 years return period wave event at the plateau, given by wave condition $H_s = 12.5$ m and $T_p = 15.2$ s. Not only the 100 years return period wave event were simulated in order to allow comparisons between laboratory data and field measured from the pilot plant once built. The wave signals were stored and reused from transducer configuration number one to configuration number two. Each of the 32 tests was thereby performed twice.

| Test | H_s [m] | T_p [s] | swl [m] | Direction | Wave field | n |
|------|--------------|--------------|------------|-----------|---------------|----|
| 1 | 0.125 | 1.55 | 0.50 | Front | 2D | - |
| 2 | 0.167 | 1.81 | 0.50 | Front | 2D | - |
| 3 | 0.208 | 1.94 | 0.50 | Front | 2D | - |
| 4 | 0.250 | 2.07 | 0.50 | Front | 2D | - |
| 5 | 0.042 | 1.03 | 0.50 | Side | 2D | - |
| 6 | 0.083 | 1.29 | 0.50 | Side | 2D | - |
| 7 | 0.125 | 1.55 | 0.50 | Side | 2D | - |
| 8 | 0.167 | 1.81 | 0.50 | Side | 2D | - |
| 9 | 0.125 | 1.55 | 0.53 | Front | 2D | - |
| 10 | 0.167 | 1.81 | 0.53 | Front | 2D | - |
| 11 | 0.208 | 1.94 | 0.53 | Front | 2D | - |
| 12 | 0.250 | 2.07 | 0.53 | Front | 2D | - |
| 13 | 0.042 | 1.03 | 0.53 | Side | 2D | - |
| 14 | 0.083 | 1.29 | 0.53 | Side | 2D | - |
| 15 | 0.125 | 1.55 | 0.53 | Side | 2D | - |
| 16 | 0.167 | 1.81 | 0.53 | Side | 2D | - |
| 17 | 0.125 | 1.55 | 0.53 | Front | 3D | 4 |
| 18 | 0.167 | 1.81 | 0.53 | Front | 3D | 4 |
| 19 | 0.208 | 1.94 | 0.53 | Front | 3D | 4 |
| 20 | 0.250 | 2.07 | 0.53 | Front | 3D | 4 |
| 21 | 0.042 | 1.03 | 0.53 | Side | 3D | 4 |
| 22 | 0.083 | 1.29 | 0.53 | Side | 3D | 4 |
| 23 | 0.125 | 1.55 | 0.53 | Side | 3D | 4 |
| 24 | 0.167 | 1.81 | 0.53 | Side | 3D | 4 |
| 25 | 0.125 | 1.55 | 0.53 | Front | 3D | 10 |
| 26 | 0.167 | 1.81 | 0.53 | Front | 3D | 10 |
| 27 | 0.208 | 1.94 | 0.53 | Front | 3D | 10 |
| 28 | 0.250 | 2.07 | 0.53 | Front | 3D | 10 |
| 29 | 0.042 | 1.03 | 0.53 | Side | 3D | 10 |
| 30 | 0.083 | 1.29 | 0.53 | Side | 3D | 10 |
| 31 | 0.125 | 1.55 | 0.53 | Side | 3D | 10 |
| 32 | 0.167 | 1.81 | 0.53 | Side | 3D | 10 |

Table 1. Summary of model wave conditions.

2 Loading conditions

Previous works by Allsop et al. (1996), Calabrese and Vicinanza (1999), Vicinanza (1999) show how the forms and magnitudes of wave pressures acting upon caisson breakwaters under random wave conditions are highly variable and they are divided into “pulsating”, when they are slowly-varying in time and the pressure spatial gradients are mild, and “impact”, when they are rapidly-varying in time and the pressure spatial gradients are extremely high

Two principal quasi-static loadings may be considered here. First, a wave crest impinges directly against the structure applying a hydro-static pressure difference. The obstruction of the momentum of the wave causes the wave surface to rise up the wall, increasing the pressure difference across the plates; the net force is approximately proportional to the wave height, and can be estimated using relatively simple methods. Wave impacts occurs when the waves break directly on the structure with almost vertical front surface at the moment of impact or as a plunging breaker with cushion of air inducing loads of much greater

intensity and shorter duration than the quasi-static loads (Figure 4).

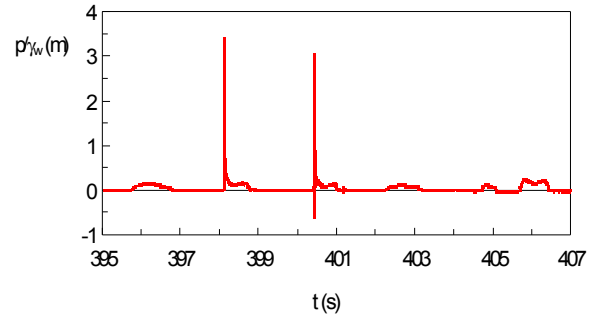


Figure 4: Quasi-static and impact pressure time history (after Vicinanza, 1999).

A preliminary visual test analysis (Fig. 5) permitted to identify two different behaviors of waves acting on the structure:

- surging waves, characterized by a rapid rise of the wave along the three sloping front caisson plates – no breaking waves;

- impact of water jet, resulting from massive wave overtopping directly hitting the vertical rear wall in upper reservoir, characterized by evident wave slamming.

Because of this different wave-structure interactions two different pressure sampling rate were set up. Each test was run twice. On the first run pressure data were acquired at a rate of 200 Hz. A second run was carried out at sampling rate of 1200 Hz.

4 Results of pressures on the structure

The first part of the experimental data analysis was finalized to identify the loading regime on different structure locations. In Figure 6 an example of pressure time history recorded by transducers mounted on the front sloping walls under normal extreme wave attack is shown. It should be noted that the generated wave pressures shows higher values on the central plate 2. A quasi-static loading time history is recognizable over all the front side plates and the pressure is almost hydrostatic ($p \approx p_w$ g Hm).

It should be noted that the generated wave pressures do not vary substantially from one plate to another. Thus, a quasi-static loading time history is recognizable.

The shape of the spatial pressure distribution on the front plates is shown in Figure 7. The non-dimensional pressure is plotted against the transducer position at time of the maximum pressure on plate 2. The pressure distribution assumes a typical trapezoidal shape (Goda, 1974; Goda, 1985). A completely different behaviour was recognized from time history analysis of the pressure transducer at the rear wall in the upper reservoir (Fig.8). Comparison with front plate transducer signal show evident rapidly-varying in time and high pressure peaks typically described as “impact” ($p \approx 4 p_w$ g Hm). This pressure example exhibits a relative small impact pressure due to the damped breaking waves (impacts pressures can be up to $p \approx 50 - 100 p_w$ g Hm).

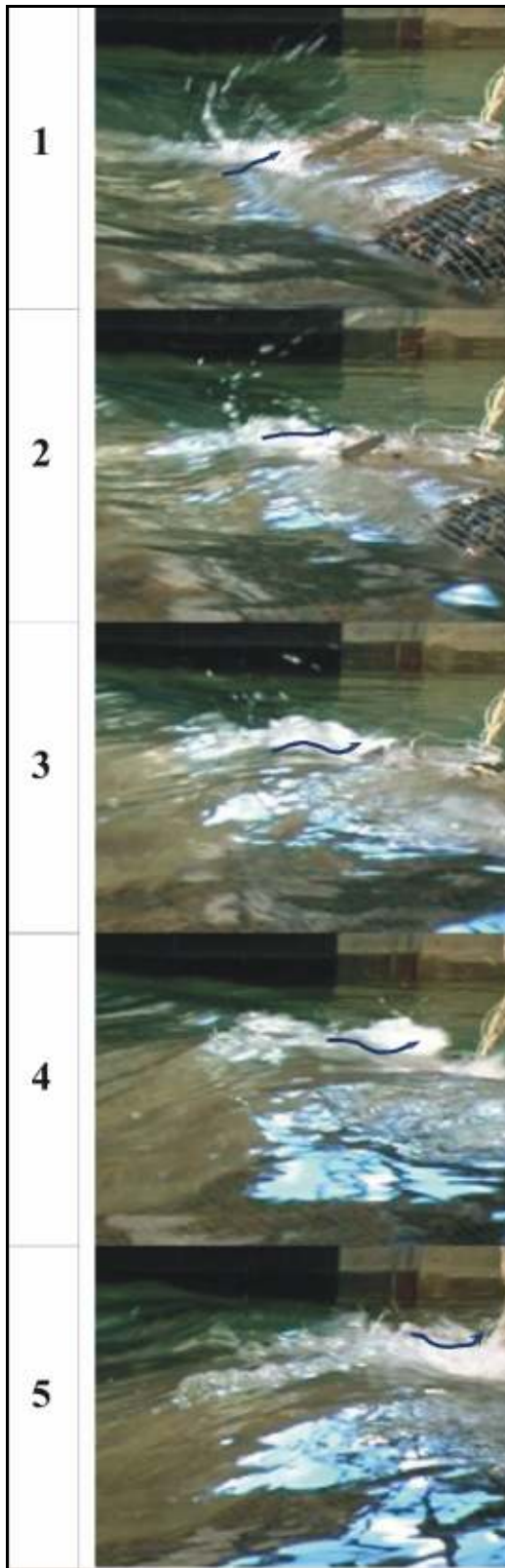


Figure 5: Sequence of video frames from test 4 (time between frames: 0.2 s).

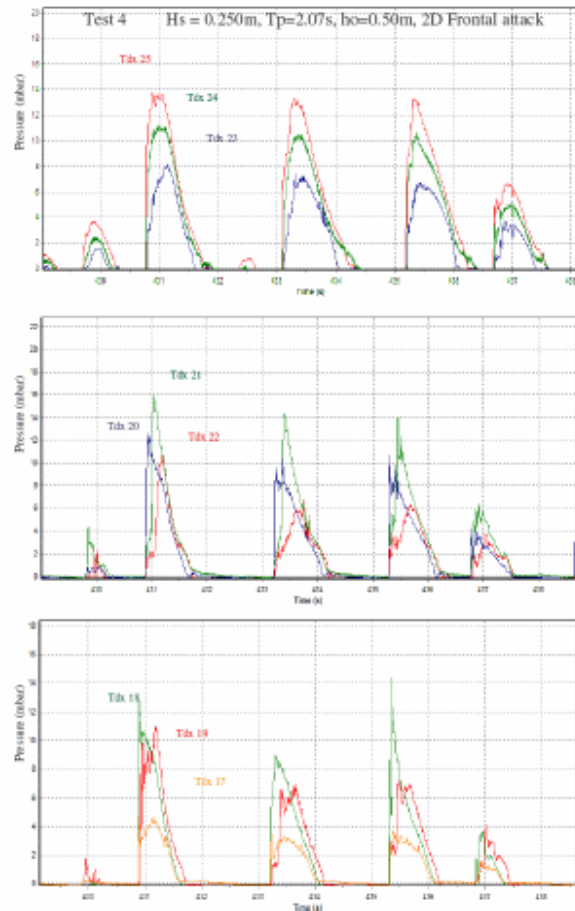


Figure 6: Pressure time history at the transducers on the front plates.

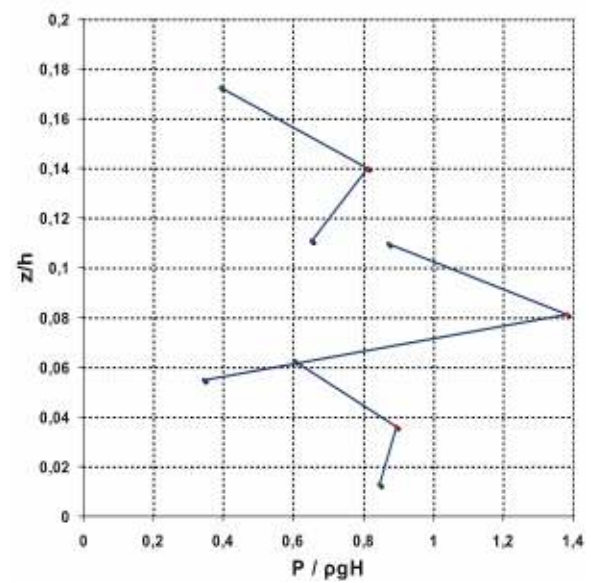


Figure 7: Maximum pressure spatial distribution at the transducers on the front plates.

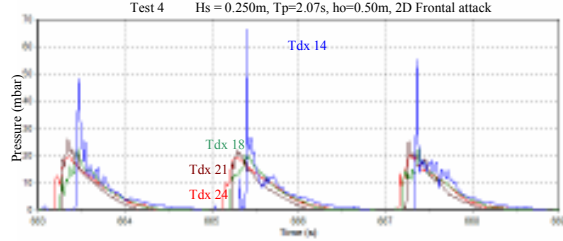


Figure 8: Comparison between transducer on the front plate and on the rear wall.

The major emphasis in any study on wave loadings is on the overall or average level of pressures, which is needed to determine the overall stability of the structure. Data on local pressures and pressure gradients are also needed in any analysis of conditions leading to local damage. The results appear to indicate that pressures on front plates are quasi static ($p_1/250 \sim \rho_w g H_{max}$) or pulsating loads generated by non-breaking waves. The wave loading on the rear vertical wall are varying over 2 - 3 $\rho_w g H_{max}$. In this case the wave is collapsing in the upper reservoir in front of the wall. This loading case exhibits a relative small impact pressure due to the damped breaking waves.

The analysis of these pressure measurements made at laboratory scale using fresh water has explicitly assumed a Froude scale conversion to prototype values. In the case of pulsating wave pressures the assumption of Froude scaling is realistic while for wave impact pressure scaling is less simple. It has long been argued in the EU project on caisson breakwaters, PROVERBS (Oumeraci et al., 1999), that wave impact in small scale hydraulic model tests will be greater in magnitude, but shorter in duration than their equivalents at full scale in (invariably aerated) sea water. It is very probable that the higher peak pressures measured in these model tests can be scaled to lower values, but probably each will attend by longer impulse durations. The argument on scaling these peak pressures requires information not presently available on the relationships between the statistics of the pressure time gradients and the magnitude of the pressure impulses. It can be argued that the magnitude of the pressure impulse, given perhaps by ($p \Delta t$) will not be changed between model and prototype, other than by the normal scaling relationships. Measurements of wave pressures planned at pilot SSG in Kvitsøy will be useful to estimate model-prototype scaling discrepancies.

5 Overtopping tests

The present section investigates the phenomena responsible of the reduction of efficiency passing from 2D laboratory conditions to 3D conditions.

These are:

- Directionality.
- Spreading.
- 3D-ness of the structure (boundary effects, not optimal slope leading to the model...).

The objective was to estimate the hydraulic efficiency

of the SSG pilot.

The last point has been investigated with a comparison between 2D waves in the described setup and 2D waves in a 2D setup of earlier tests not described in this work (Kofoed 2005); the result of that study indicates an hydraulic efficiency for the SSG pilot of 50%.

Each test was of approximately 1500 waves in normal operational conditions ($H_s < 7.4$ m and 6.1 s $< T_p < 12.7$ s). Tests have been carried out with attack angles varying between -15° and 15° (directions between 255° and 285° at the pilot location), 8 spreading conditions and 3 water levels. Spreading and directionality were investigated separately. The directional spreading (n) function adopted is expressed by the following form:

$$\cos^{2n} |(\beta - \beta_0) / 2|$$

The rear part of model was modified and equipped with four slopes leading to different small tank containers: one for each reservoir plus one for the overtopping of the whole structure (Figure 9). In this way the front part was the same as the loading tests (Section 1). The captured overtopping water was then temporally stored and then pumped out again in the basin by small pumps of known capacity; the pumps were automatically activated when the water inside the single containers was reaching a certain pre-established level. By the total utilization of the pumps and the records of water levels inside the rear tanks, the overtopping flow rates have been derived for the single reservoirs. The hydraulic efficiency has been defined and calculated as the ratio between the power in the overtopping water (P_{crest}) and the power in incoming waves (P_{wave}):

$$P_{crest} = \sum_{j=1}^3 q_{ov,j} R_{C,j} \rho g$$

$$P_{wave} = \frac{\rho g^2}{64\pi} H_s^2 T_E$$

The measuring equipment included:

1. 4 wave gauges installed to measure time series of water levels in the reservoirs tanks.
2. 7 resistive wave probes on a pentangle array placed on the plateau in front of the model, enabling the collection of data for 3D wave analysis.



Figure 9: Model for 3D overtopping tests.

3 Overtopping results

In Figure 10 flow rates of the tests for the 3 reservoirs (q_1 , q_2 and q_3) are plotted for different spreading conditions; reservoir number 1 is the lower, while nr. 2 and 3 are the middle and higher ones. The results appear grouped in the graphics depending on the wave high (increasing with H_s). While little difference can be noticed comparing the 2D and the different spreading conditions in reservoir one and two, in reservoir number three for higher H_s the difference between tests with low spreading (\approx 2D conditions) and high spreading are relevant. In Figure 11 the calculated efficiency of laboratory tests with and without spreading is plotted against the efficiency with spreading divided the efficiency without spreading. In black the overall trend of the results depending on spreading. A local effect regards the W2 condition and it could be imputable to the different interaction of the specific short period of the waves with the bathymetry.

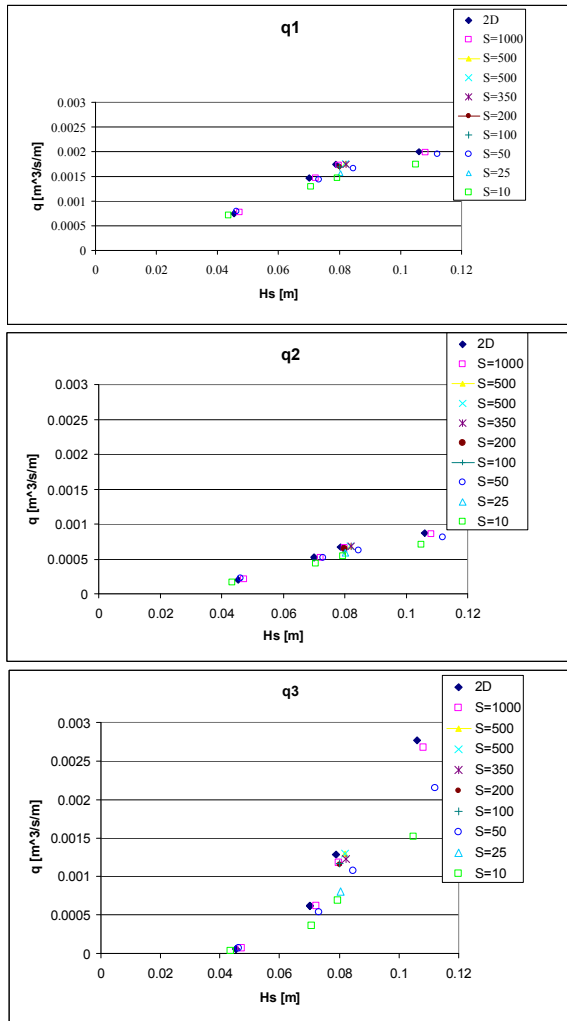


Figure 10: Flow rates into the 1st, 2nd and 3rd reservoir for different wave heights and input spreading coefficients.

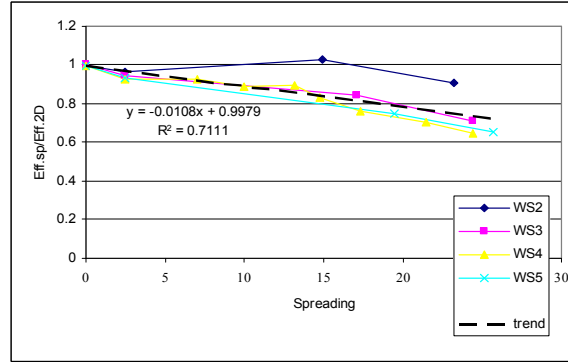


Figure 11: Tests results from laboratory plotted against the efficiency with spreading (2D conditions) divided by the efficiency without spreading. The results are plotted for 4 different wave conditions.

In figure 12 the flow rates for the three reservoirs are plotted for different attack angles ($\theta = 0^\circ$ = direct attack). Again little difference can be noticed in reservoir 1 and 2 by increasing θ for the same H_s , while in reservoir number three the flow rates (q_3) are very influence by the directionality. A local effect can also be distinguished by a closer look to the graphic: for the same wave highs waves with a positive attack angle ($+\theta$) give a bigger flow rate in the 3rd reservoir than the ones with a negative attack angle ($-\theta$) and comparable absolute value. This is probably due to the influence of the bathymetry which has a steep slope or focusing characteristics on the left part of the structure (facing the sea). This asymmetry of results is even more evident when plotting the efficiency.

In Figure 13 the calculated efficiency of laboratory tests with and without directionality is plotted against the efficiency with directionality divided the efficiency without directionality. Again the W2 condition behaves weirdly when adding an attack angle but all the tests present is an asymmetry of the results. Not all the range of attack angles has been tested; in reality at the selected SSG pilot location the attack angle can be $\pm 40^\circ$ while in the laboratory only an attack angles up to $\pm 15^\circ$ have been tested. It is anyway suggested that the efficiency can not decrease to 0 while increasing the attack angle in a range between $\pm 40^\circ$. What it is expected to happened in that case, is that local phenomena will convert the waves to the structure and the efficiency will converge to a low threshold. For this reason the trend of the red line in Figure 13 is suggested for the location tested in laboratory. The asymmetric effect still present but a limit has been set up for the lowest decrease of efficiency from the 2D conditions; the reduction of efficiency has been estimated to be of 0.6 for the NW directions while 0.45 for the SW directions.

The results from the laboratory tests indicate a decrease of efficiency from 50% in 2D conditions:

- to 40% due to 3D characteristic of the structure (as expected).
- to 30% (severe spreading). Spreading coming with waves can not be avoided and depending on its magnitude, it can decrease the hydraulic efficiency of the pilot project. In average it can be

said that spreading decreases efficiency up to 32%.

- to 25% for unfavorable attack angle on the structure. The influence of directionality is difficult to classify as strictly dependent on the bathymetry of the area and different wave conditions interact differently with the bottom; in average it can be said that directionality decreases efficiency up to 35%.

The combination of 3D-ness, spreading and directionality in the most severe condition decreases the efficiency of the SSG pilot from 50% to 15%. In average the overall decrease would be from 50% to 25%. These results are valid for the SSG pilot that has a very low width to depth ratio and it is therefore extremely sensitive to spreading and directionality. On a different configuration (more modules on a breakwater) those negative effects are milder.

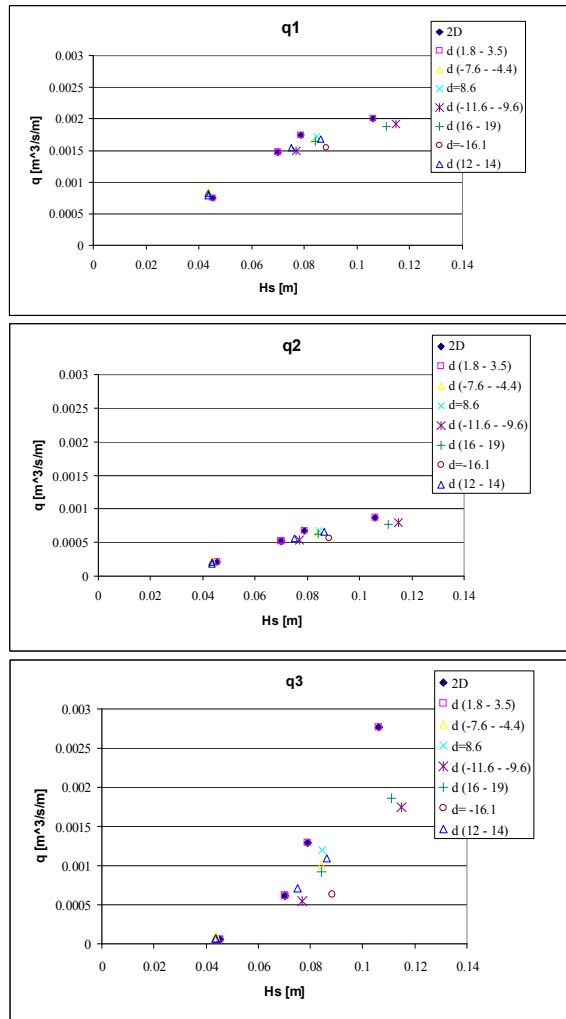


Figure 12: Flow rates into the 1st, 2nd and 3rd reservoir for different wave heights and input spreading coefficients.

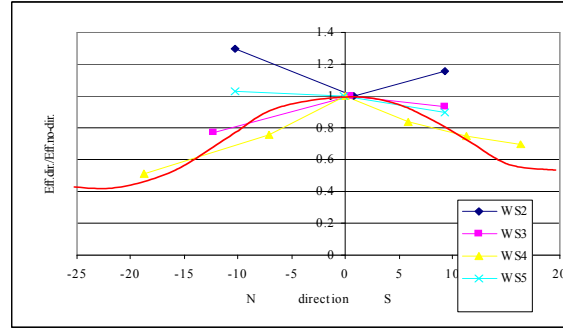


Figure 13: Flow rates into the 1st, 2nd and 3rd reservoir for different wave heights and input spreading coefficients and suggested trend of normalized efficiency depending on attack angle at the SSG structure (selected location).

3 Conclusions

The results of some recent research regarding a new type of structure for wave energy conversion Seawave Slot-Cone Generator (SSG) have been reviewed and discussed. For the first time at the Aalborg University the SSG concept has been modelled and tested with the main aim to give advice on expected overtopping rates and power production and on the structure designers on wave loading acting on different parts of the structure. Mainly two different behaviours were identified: surging waves on the front sloping plates and damped impact water jet on the vertical rear wall in upper reservoir. The order of magnitude of the extreme peak pressure on the front plates scaled to prototype were up to 250 kN/m². On the vertical rear wall in the upper reservoir impact pressures (very peaked, short duration) of up to 580 kN/m² were registered. For wave impact pressure scaling (vertical rear wall) some prototype measurements are needed. Wave pressures measurements planned at pilot SSG in Kvitsoy will be useful to estimate model-prototype scaling discrepancies.

Additionally has been shown and discussed how 3D phenomena are expected to reduce the hydraulic efficiency estimated to be around 50% in 2D studies, to 25%. This is mainly due to the spreading and the directionality that are reducing the overtopping flow rates inside the reservoirs and so the stored potential energy. This is a result valid for the SSG pilot that is a module with a low width to depth ratio: when an attack angle is present, it has been noticed that waves hit the side walls and part of the water finds an obstacle to enter the reservoirs.

From these results the following conclusions have been reached:

1. a reduction of efficiency from 50% (2D conditions) to 40% due to the 3D-ness of the structure has been calculated.

2. A reduction of efficiency from 50% (2D conditions) to 32% due to spreading has been calculated.
3. A reduction of efficiency 50% (2D conditions) to 35% due to directionality has been calculated.
4. A reduction of efficiency from 50% (2D conditions) to 25% due to the combination of 3d-ness, spreading and directionality has been calculated.
5. The negative spreading effect on the efficiency increases with the increase of the spreading.
6. The negative directionality effect on the efficiency increases with the increase of the attack angle.
7. Prove of the influence of the bathymetry has been highlighted: waves with a positive attack angle (SW) have less negative influence on the flow rates and on the efficiency than the corresponding waves with a negative attack angle (NW).

References

- [1] J. P. Kofoed. *Vertical Distribution of wave overtopping for design of multilevel overtopping based wave energy converter*. International Conference on Coastal Engineering, San Diego, US, 2006.
- [2] D. Vicinanza, J. P. Kofoed, and P. Frigaard. *Wave loadings on Seawave Slot-cone Generator (SSG) at Kvitsøy island (Stavanger, Norway)*. Hydraulics and Coastal Engineering No. 35, ISSN: 1603-9874, Dep. of Civil Eng., Aalborg University, 2006.
- [3] N. W. H. Allsop, D. Vicinanza & J. E. McKenna. *Wave forces on vertical and composite breakwaters*. Strategic Research Report, Hydraulic Research Wallingford, Sr 443, Wallingford 1996.
- [4] M. Calabrese, D. Vicinanza. *Prediction of wave impact occurrence on vertical and composite breakwaters*. Excerpta of Italian contributions to the field of hydraulic engineering, Vol. XIII, 25pp., ISSN 0394-526X, 1999.
- [5] D. Vicinanza. *Breaking wave kinematics in front of composite breakwaters*. Proceedings of the International Conference Coastal Structures, Santander, Spain, 1999.
- [6] Y. Goda. *New Wave Pressure Formulae for Composite Breakwaters*. Proceedings of the 14th International Coastal Engineering Conference, Vol 3, pp 1702-1720, 1974.
- [7] Y. Goda. *Random Seas and Design of Maritime Structures*. University of Tokyo Press, Tokyo, Japan, 1985.
- [8] H. Oumeraci, P. Klammer & H. W. Partenscky. *Classification of breaking wave loads on vertical structures*. Proc. ASCE, J. Waterw. Port Coastal Ocean Eng. Div., 119 (4), 1993.
- [9] J. P. Kofoed. *Model testing of the wave energy converter Seawave Slot-Cone Generator*. Hydraulic and Coastal Engineering No. 18, ISSN 1603-9874, Dep. Of Civil Eng., Aalborg University, 2005.